Proceedings of the Canadian Society for Mechanical Engineering International Congress 2021
CSME Congress 2021
June 27-30, 2021, Charlottetown, PE, Canada

Fault Detection of a Mechatronic System using Interacting Operating Modes

S. Andrew Gadsden[1,*], Stephen A. Wilkerson[2], Mohammad Al-Shabi[3]
[1]College of Engineering and Physical Sciences, University of Guelph, Guelph, Canada
[2]Department of Mechanical Engineering, York College of Pennsylvania, York, USA
[3]Department of Mechanical and Nuclear Engineering, University of Sharjah, Sharjah, UAE
*gadsden@uoguelph.ca

Abstract—Successful fault detection and diagnosis is important for reliable operation of engineering systems. A number of strategies exist, utilizing both signal-based and model-based methods. The interacting multiple model (IMM) strategy is one of the most well-established methods to distinguish between different operating modes. The IMM utilizes estimation filters that run in parallel based on different models that describe or capture the system dynamics or behaviour. In this paper, a number of different estimation strategies have been combined with the IMM for fault detection and diagnosis of a mechatronic system. This paper studies the most popular methods, and compares the fault detection results of an electrohydrostatic actuator (EHA) that was built for experimentation.

Keywords-Fault detection; interacting multiple model; control; mechatronics; estimation theory

I. INTRODUCTION

Fault detection and diagnosis strategies are used to ensure the reliable and safe operation of different engineering systems. They are part of the controls systems engineering field, and includes: system health and condition monitoring, identifying when faults occur, and diagnosing the type of fault. A fault is defined as an abnormal condition that may lead system deviation from its normal operating conditions. Some of the most popular research in this area includes: books [1, 2, 3, 4, 5], research theses [6, 7, 8], and other survey papers [9, 10, 11, 12, 13, 14, 15, 16, 17, 18]. A number of different types of FDI strategies exist, and are usually classified as model-based or signal-based. The most well-known signal-based strategy is based on artificial neural network (ANN) techniques. The most well-studied model-based strategy is the interacting multiple model (IMM) method. In order to properly implement these strategies, knowledge on the system states and parameters is required. State estimation-based methods are considered to be an important branch of fault diagnosis, and have attracted a significant amount of attention in recent years.

The most popular estimation method for linear systems and measurements remains the Kalman filter (KF) [19, 20]. It yields a statistical optimal solution to the estimation problem (with linear systems and measurements), under strict assumptions. For the nonlinear cases, a number of KF-based strategies have been created, and include: the extended (EKF), unscented (UKF), and cubature Kalman filter (CKF) [8]. Note that the CKF is a special case of the UKF [8]. These strategies attempt to approximate the nonlinearities through linearization, the use of sigma-points, or particles like the particle filter (PF) [21]. Another strategy derived based on variable structure techniques is the smooth variable structure filter (SVSF), which was presented in an effort to overcome instability issues found in the KF-based methods [22]. Most recently, an estimation strategy called the sliding innovation filter (SIF) was introduced in [23]. Although similar structure to the SVSF, the SIF presents a simpler gain and yields a more accurate estimate.

This study compares the IMM fault detection and diagnosis strategy, combined with the EKF, UKF, CKF, PF, and SVSF estimation methods. An electrohydrostatic actuator (EHA) that was built for experimentation is used to test out and compare the different IMM strategies. The paper is organized as follows. An overview of the IMM strategy is provided in Section 2. Section 3 lists the main equations for the estimation methods. Section 4 describes the experimental setup and the corresponding results. The main findings and conclusions are then summarized in Section 5.

II. INTERACTING MULTIPLE MODEL STRATEGY

This section provides a general overview of the IMM strategy. A comprehensive explanation of the IMM estimator with its application to multiple model target tracking was presented by Bar-Shalom et al. in [24]. Furthermore, a significant amount of research has been presented which combined the IMM with filtering strategies such as the EKF [25], PF [26, 27], SVSF [28], and the Dempster-Shafer data association technique [29]. The IMM's main feature includes the ability to estimate the state of a system which can be modeled using a finite number of mathematical models, and can 'switch' from one mode to another based on its likelihood function (probability) [30]. The IMM method consists of three main steps, as defined in [31]: interaction, filtering, and combination.

The first step in the IMM process is referred as the interaction step, and it involves calculation of mixing probabilities $\mu_{i|j,k|k}$. These values are based on the probability of the system switching from mode i to the other mode j, or staying in the same mode i, at the next time step. The mixing

probabilities or likelihoods are calculated using the following equations [24]:

$$\mu_{i|j,k|k} = \frac{1}{\bar{c}_j} p_{ij} \mu_{i,k} \tag{2.1}$$

$$\bar{c}_j = \sum_{i=1}^{r} p_{ij}\, \mu_{i,k} \tag{2.2}$$

A list of the nomenclature is provided in the Appendix. The previous mode-matched states $\hat{x}_{i,k|k}$ and state error covariance's $P_{i,k|k}$ are also used to calculate the mixed initial conditions. These conditions are used as inputs for the filter matched to M_j (which includes A_j and B_j). The mixed initial conditions (state estimates and error covariance's) are found as follows [24]:

$$\hat{x}_{0j,k|k} = \sum_{i=1}^{r} \hat{x}_{i,k|k} \mu_{i|j,k|k} \tag{2.3}$$

$$P_{0j,k|k} = \sum_{i=1}^{r} \mu_{i|j,k|k} \{ \dots$$

$$P_{i,k|k} + \left(\hat{x}_{i,k|k} - \hat{x}_{0j,k|k}\right)\left(\hat{x}_{i,k|k} - \hat{x}_{0j,k|k}\right)^T \} \tag{2.4}$$

This step is interchangeable based on the estimation method that was used with the IMM strategy. For completeness, the KF steps will be described here. The state estimates $\hat{x}_{0j,k|k}$ (2.3) and corresponding covariance $P_{0j,k|k}$ (2.4) for each model j are used to predict the estimate $\hat{x}_{j,k+1|k}$ (2.5) and calculate the predicted error covariance $P_{j,k+1|k}$ (2.6).

$$\hat{x}_{j,k+1|k} = A_j \hat{x}_{0j,k|k} + B_j u_k \tag{2.5}$$

$$P_{j,k+1|k} = A_j P_{k|k}^{0j} A_j^T + Q_k \tag{2.6}$$

The mode-matched innovation covariance $S_{j,k+1|k}$ (2.7) and predicted measurement error (or innovation) $e_{j,z,k+1|k}$ (2.8) are calculated respectively as follows:

$$S_{j,k+1|k} = C_j P_{j,k+1|k} C_j^T + R_{k+1} \tag{2.7}$$

$$e_{j,z,k+1|k} = z_{k+1} - C_j \hat{x}_{j,k+1|k} \tag{2.8}$$

Following this, the mode-matched gain $K_{j,k+1}$ (e.g., KF) is calculated as per (2.9), and then used to update the estimates $\hat{x}_{j,k+1|k+1}$ as per (2.10). The state error covariance $P_{j,k+1|k+1}$ is updated using (2.11) and the measurement error $e_{j,z,k+1|k+1}$ is updated as per (2.12).

$$K_{j,k+1} = P_{j,k+1|k} C_j^T S_{j,k+1|k}^{-1} \tag{2.9}$$

$$\hat{x}_{j,k+1|k+1} = \hat{x}_{j,k+1|k} + K_{j,k+1} e_{j,z,k+1|k} \tag{2.10}$$

$$P_{j,k+1|k+1} = \left(I - K_{j,k+1} C_j\right) P_{j,k+1|k} \tag{2.11}$$

$$e_{j,z,k+1|k+1} = z_{k+1} - C_j \hat{x}_{j,k+1|k+1} \tag{2.12}$$

A mode-matched likelihood function $\Lambda_{j,k+1}$ may be calculated next, as follows [24, 32]:

$$\Lambda_{j,k+1} = \mathcal{N}\left(z_{k+1}; \hat{z}_{j,k+1|k}, S_{j,k+1}\right) \tag{2.13}$$

$$\Lambda_{j,k+1} = \frac{1}{\sqrt{\left|2\pi S_{j,k+1}\right|_{Abs}}} exp\left(\frac{-\frac{1}{2} e_{j,z,k+1|k}^T e_{j,z,k+1|k}}{S_{j,k+1}}\right) \tag{2.14}$$

The mode-matched likelihood values $\Lambda_{j,k+1}$ are used to update the mode probability $\mu_{j,k}$ by [24]:

$$\mu_{j,k} = \frac{1}{c} \Lambda_{j,k+1} \sum_{i=1}^{r} p_{ij}\, \mu_{i,k} \tag{2.15}$$

$$c = \sum_{j=1}^{r} \Lambda_{j,k+1} \sum_{i=1}^{r} p_{ij}\, \mu_{i,k} \tag{2.16}$$

In this final step, the IMM state estimates $\hat{x}_{k+1|k+1}$ (2.17) and corresponding error covariance $P_{k+1|k+1}$ (2.18) are calculated.

$$\hat{x}_{k+1|k+1} = \sum_{j=1}^{r} \mu_{j,k+1} \hat{x}_{j,k+1|k+1} \tag{2.17}$$

$$P_{k+1|k+1} = \sum_{j=1}^{r} \mu_{j,k+1} \{ P_{j,k+1|k+1} +$$

$$\dots \left(\hat{x}_{j,k+1|k+1} - \hat{x}_{k+1|k+1}\right)\left(\hat{x}_{j,k+1|k+1} - \hat{x}_{k+1|k+1}\right)^T \} \tag{2.18}$$

Note that this step is used for the overall IMM output, and is not used recursively in the process [24].

III. Estimation Strategies

The main equations for the EKF, UKF, CKF, PF, and SVSF estimation methods are summarized in this section. The extended Kalman filter (EKF) was introduced to implement the KF in a nonlinear framework. The filter is essentially the same as (2.5) through (2.12), except that the linear matrices A, B, and C are linearized using the nonlinear system and measurement functions f and h. For example, the linearized matrices are calculated using the following Jacobians [33]:

$$A_j = \left.\frac{\partial f_j}{\partial x}\right|_{\hat{x}_{k|k}, u_k} \tag{3.1.1}$$

$$C_j = \left.\frac{\partial h_j}{\partial x}\right|_{\hat{x}_{k+1|k}} \tag{3.1.2}$$

The linearization process can lead to uncertainties that cause the EKF to yield numerically unstable results [34]. However, for most mildly nonlinear systems, the EKF provides reliable state estimates and higher-order estimates are not needed [33].

The unscented Kalman filter (UKF) utilizes a nonlinear sampling technique known as the unscented transform [35, 36]. Equations (3.2.1) through (3.2.16) represent the UKF estimation process, and are implemented recursively [36]. The first step involves calculating what are known as 'sigma points'. In the UKF framework $2n + 1$ sigma points may be used to approximate the nonlinearities, where n refers to the number of states [36]. The initial sigma points (which include both the sample and weight) are calculated using the following two equations, respectively:

$$X_{0,k|k} = \hat{x}_{k|k} \tag{3.2.1}$$

$$W_0 = \frac{\kappa}{n+\kappa} \tag{3.2.2}$$

The next n set of sigma points are calculated using (3.2.3) and (3.2.4).

$$X_{i,k|k} = \hat{x}_{k|k} + \left(\sqrt{(n+\kappa)P_{k|k}}\right)_i \tag{3.2.3}$$

$$W_i = \frac{1}{2(n+\kappa)} \tag{3.2.4}$$

The remaining n set of sigma points are calculated using (3.2.5) and (3.2.6).

$$X_{i+n,k|k} = \hat{x}_{k|k} - \left(\sqrt{(n+\kappa)P_{k|k}}\right)_i \tag{3.2.5}$$

$$W_{i+n} = \frac{1}{2(n+\kappa)} \tag{3.2.6}$$

The parameter κ in the above is a design value (typically a positive value less than 1), the second term in (3.2.5) is the i^{th} row or column of $\sqrt{(n+\kappa)P_{k|k}}$ which is a matrix, and W_i refers to the weight associated with the i^{th} sample point [37]. The sigma points calculated in (3.2.1) through (3.2.6) are propagated through the nonlinear system or measurement models, and are used to predicted state estimate (3.2.8) or predicted measurement (3.2.11).

$$\hat{X}_{i,k+1|k} = f\left(X_{i,k|k}, u_k\right) \tag{3.2.7}$$

$$\hat{x}_{k+1|k} = \sum_{i=0}^{2n} W_i \hat{X}_{i,k+1|k} \tag{3.2.8}$$

From (3.2.7) and (33.2.8), the predicted state error covariance is calculated as per the following:

$$P_{k+1|k} = \sum_{i=0}^{2n} W_i \left(\hat{X}_{i,k+1|k} - \hat{x}_{k+1|k}\right)\left(\hat{X}_{i,k+1|k} - \hat{x}_{k+1|k}\right)^T \tag{3.2.9}$$

Furthermore, the sigma points are used in the nonlinear measurement function (3.2.10) and then used to predict the measurement as per (3.2.11).

$$\hat{Z}_{i,k+1|k} = h\left(\hat{X}_{i,k+1|k}, u_k\right) \tag{3.2.10}$$

$$\hat{z}_{k+1|k} = \sum_{i=0}^{2n} W_i \hat{Z}_{i,k+1|k} \tag{3.2.11}$$

Using (3.2.10) and (3.2.11), the innovation covariance is calculated:

$$P_{zz,k+1|k} = \sum_{i=0}^{2n} W_i \left(\hat{Z}_{i,k+1|k} - \hat{z}_{k+1|k}\right)\left(\hat{Z}_{i,k+1|k} - \hat{z}_{k+1|k}\right)^T \tag{3.2.12}$$

The cross-covariance (defined as the cross-covariance between the state and measurement) is calculated as per the following:

$$P_{xz,k+1|k} = \sum_{i=0}^{2n} W_i \left(\hat{X}_{i,k+1|k} - \hat{x}_{k+1|k}\right)\left(\hat{Z}_{i,k+1|k} - \hat{z}_{k+1|k}\right)^T \tag{3.2.13}$$

From (3.2.12) and (3.2.13), the gain K_{k+1} is calculated as per (3.2.14).

$$K_{k+1} = P_{xz,k+1|k} P_{zz,k+1|k}^{-1} \tag{3.2.14}$$

The updated state estimates are calculated as per (3.2.15), and the error covariance is updated using (3.2.16).

$$\hat{x}_{k+1|k+1} = \hat{x}_{k+1|k} + K_{k+1}\left(z_{k+1} - \hat{z}_{k+1|k}\right) \tag{3.2.15}$$

$$P_{k+1|k+1} = P_{k+1|k} - K_{k+1} P_{zz,k+1|k} K_{k+1}^T \tag{3.2.16}$$

Note that for mildly nonlinear systems and measurements, the EKF and UKF yield the same solutions. However, the UKF is more advantageous when the nonlinearities are more pronounced.

The cubature Kalman filter (CKF) is similar to the UKF strategy, and has been found to be a special case of the UKF. The CKF utilizes a third-degree cubature rule to compute Gaussian-weighted integrals in an effort to solve the estimation problem [38]. The cubature rule attempts to approximate a weighted integral as follows [38]:

$$\int_{\mathbb{R}^{n_x}} f(x)\mathcal{N}\left(x; \mu, \sum\quad\right) dx \approx \frac{1}{2n} f\left(\mu + \sqrt{\sum\quad}\,\xi_i\right) \tag{3.3.1}$$

In order to maintain numerical stability, a square-root factor of the covariance $\sum$ is defined to satisfy the relationship $\sum = \sqrt{\sum}\sqrt{\sum}^T$. In this case, a set of $2n$ cubature points are defined as follows [38]:

$$\xi_i = \begin{cases} \sqrt{n}e_i, & i = 1,2,\dots,n \\ -\sqrt{n}e_{i-n}, & i = n+1, n+2, \dots, 2n \end{cases}$$

where $e_i \in \mathbb{R}^n$ refers to the i^{th} elementary column vector. Initial cubature points X are calculated using the previous time step's updated state estimate $\hat{x}_{k|k}$, the previous update error covariance $P_{k|k}$, and the cubature-point set ξ_i as per (3.3.2) [38]. Similar to the UKF process, these points are fed into the nonlinear system function (3.3.3).

$$X_{i,k|k} = \sqrt{P_{k|k}}\xi_i + \hat{x}_{k|k} \qquad i = 1,2,\dots,2n \tag{3.3.2}$$

$$X^*_{i,k+1|k} = f\left(X_{i,k|k}, u_k\right) \qquad i = 1,2,\dots,2n \tag{3.3.3}$$

The predicted state estimates $\hat{x}_{k+1|k}$ and predicted error covariance $P_{k+1|k}$ are found using (3.3.3), respectively as follows:

$$\hat{x}_{k+1|k} = \frac{1}{2n}\sum_{i=1}^{2n} X^*_{i,k+1|k} \tag{3.3.4}$$

$$P_{k+1|k} = \frac{1}{2n}\sum_{i=1}^{2n} X^*_{i,k+1|k} X^{*T}_{i,k+1|k} - \hat{x}_{k+1|k}\hat{x}^T_{k+1|k} + Q_{k+1} \tag{3.3.5}$$

As per [38], the predicted cubature points $X_{i,k+1|k}$ are calculated using (3.3.4) and (3.3.5):

$$X_{i,k+1|k} = \sqrt{P_{k+1|k}}\xi_i + \hat{x}_{k+1|k} \qquad i = 1,2,\dots,2n \quad (3.3.6)$$

Similar to the UKF process, the predicted cubature points $X_{i,k+1|k}$ are fed into the nonlinear measurements function to find $Z_{i,k+1|k}$ as per (3.3.7). Furthermore, the predicted measurements $\hat{z}_{k+1|k}$ are calculated as per (3.3.8) [38].

$$Z_{i,k+1|k} = h\big(X_{i,k+1|k}, u_{k+1}\big) \qquad i = 1,2,\dots,2n \quad (3.3.7)$$

$$\hat{z}_{k+1|k} = \frac{1}{2n}\sum_{i=1}^{2n} Z_{i,k+1|k} \quad (3.3.8)$$

The innovation covariance $P_{zz,k+1|k}$ and cross-covariance $P_{xz,k+1|k}$ matrices are calculated respectively using (3.3.9) and (3.3.10) [38].

$$P_{zz,k+1|k} = \frac{1}{2n}\sum_{i=1}^{2n} Z_{i,k+1|k}Z_{i,k+1|k}^T - \hat{z}_{k+1|k}\hat{z}_{k+1|k}^T + R_{k+1} \quad (3.3.9)$$

$$P_{xz,k+1|k} = \frac{1}{2n}\sum_{i=1}^{2n} X_{i,k+1|k}Z_{i,k+1|k}^T - \hat{x}_{k+1|k}\hat{z}_{k+1|k}^T \quad (3.3.10)$$

Finally, the corresponding CKF gain is calculated in (3.3.11), The CKF gain is used to update the states estimates in (3.3.12) and error covariance in (3.3.13).

$$K_{k+1} = P_{xz,k+1|k}P_{zz,k+1|k}^{-1} \quad (3.3.11)$$

$$\hat{x}_{k+1|k+1} = \hat{x}_{k+1|k} + K_{k+1}\big(z_{k+1} - \hat{z}_{k+1|k}\big) \quad (3.3.12)$$

$$P_{k+1|k+1} = P_{k+1|k} + K_{k+1}P_{zz,k+1|k}K_{k+1}^T \quad (3.3.13)$$

The CKF estimation consists of (3.3.1) through (3.3.13), and is computed recursively [38].

As previously discussed, the smooth variable structure filter (SVSF) is an estimated strategy based on sliding mode concepts [22]. The SVSF uses a switching gain which causes the estimates to converge within a region of the true states (also known as the existence subspace). The SVSF has been well studied, and shown to be robust and stable to uncertainties and noise, provided an upper-bound has been defined on the level of noise and unmodeled dynamics [30]. The predicted estimates $\hat{x}_{k+1|k}$ and error covariances $P_{k+1|k}$ are calculated as per (3.5.1) and (3.5.2).

$$\hat{x}_{k+1|k} = f\big(\hat{x}_{k|k}, u_k\big) \quad (3.5.1)$$

$$P_{k+1|k} = AP_{k|k}A^T + Q_{k+1} \quad (3.5.2)$$

Note that for the covariance calculations in (3.5.2) and (3.5.7), the nonlinear system and measurement functions are linearized using Jacobian matrices, similar to the EKF [8]. The predicted measurements $\hat{z}_{k+1|k}$ and corresponding measurement errors (innovation) $e_{z,k+1|k}$ are calculated next:

$$\hat{z}_{k+1|k} = h\big(\hat{x}_{k+1|k}, u_{k+1}\big) \quad (3.5.3)$$

$$e_{z,k+1|k} = z_{k+1} - \hat{z}_{k+1|k} \quad (3.5.4)$$

As per (3.5.5), the SVSF gain is based on the predicted and previously updated measurement errors $e_{z,k+1|k}$ and $e_{z,k|k}$, boundary layer widths ψ, convergence rate γ, and the linearized (or linear) measurement matrix C [8].

$$K_{k+1} = C^+ diag\left[\left(\left|e_{z_{k+1|k}}\right| + \gamma\left|e_{z_{k|k}}\right|\right) \circ sat\left(\bar{\psi}^{-1}e_{z_{k+1|k}}\right)\right] \dots$$
$$\dots diag\left(e_{z_{k+1|k}}\right)^{-1} \quad (3.5.5)$$

The state estimates $\hat{x}_{k+1|k+1}$ and error covariance matrix $P_{k+1|k+1}$ are updated using the SVSF gain, respectively as follows:

$$\hat{x}_{k+1|k+1} = \hat{x}_{k+1|k} + K_{k+1}e_{z,k+1|k} \quad (3.5.6)$$

$$P_{k+1|k+1} = (I - K_{k+1}C)P_{k+1|k}(I - K_{k+1}C)^T + \cdots$$
$$\dots K_{k+1}R_{k+1}K_{k+1}^T \quad (3.5.7)$$

The estimated measurement $\hat{z}_{k+1|k+1}$ and corresponding measurement errors $e_{z,k+1|k+1}$ are updated, and are used in the next time step, as per the following:

$$\hat{z}_{k+1|k+1} = h\big(\hat{x}_{k+1|k+1}\big) \quad (3.5.8)$$

$$e_{z,k+1|k+1} = z_{k+1} - \hat{z}_{k+1|k+1} \quad (3.5.9)$$

The existence subspace is defined by the estimated level of uncertainties (modeling and noise) in the estimation process. Within the existence subspace, the SVSF gain causes the estimate to move and switch about the true system trajectory [39]. This high-switching is known as chattering, and brings an inherent amount of robustness to the SVSF strategy [8].

IV. Experimental Setup and Results

The electrohydrostatic actuator (EHA) is a type of aerospace actuator used for control of flight surfaces [40]. The EHA can be modelled using four states: the actuator position $x_1 = x$, velocity $x_2 = \dot{x}$, acceleration $x_3 = \ddot{x}$, and differential pressure across the actuator $x_4 = P_1 - P_2$. The physical modeling approach was used to obtain the nonlinear state-space equations in discrete-time described by [40, 41]:

$$x_{1,k+1} = x_{1,k} + Tx_{2,k} \quad (4.1)$$

$$x_{2,k+1} = x_{2,k} + Tx_{3,k} \quad (4.2)$$

$$x_{3,k+1} = 1 - \left[T\frac{a_2V_0 + M\beta_eL}{MV_0}\right]x_{3,k} - T\frac{\left(A_E{}^2 + a_2L\right)\beta_e}{MV_0}x_{2,k} \dots$$
$$\dots - T\frac{2a_1V_0x_{2,k}x_{3,k} + \beta_eL\left(a_1x_{2,k}{}^2 + a_3\right)}{MV_0}sgn\left(x_{2,k}\right)$$
$$\dots + T\frac{A_E\beta_e}{MV_0}u \quad (4.3)$$

$$x_{4,k+1} = \frac{a_2}{A_E}x_{2,k} + \frac{\left(a_1x_{2,k}{}^2 + a_3\right)}{A_E}sgn\left(x_{2,k}\right) + \frac{M}{A_E}x_{3,k} \quad (4.4)$$

The system input is defined as follows:

$$u = D_p\omega_p - sgn(P_1 - P_2)Q_{L0} \quad (4.5)$$

where ω_p is the pump speed. The definitions and numeric values of the parameters in the state space equations are found in [40].

The EKF, UKF, CKF, PF, and SVSF estimation strategies (as described earlier) were combined with the IMM method and applied on an EHA for the purposes of fault detection and diagnosis. The results are shown in this section. The following three figures illustrate the normal mode, leakage fault, and friction fault probability calculations. Furthermore, Tables 1 through 5 summarize the probability results for each method. These are referred to as confusion matrices, and provide an indication of how accurate the models were in detecting the correct operating mode.

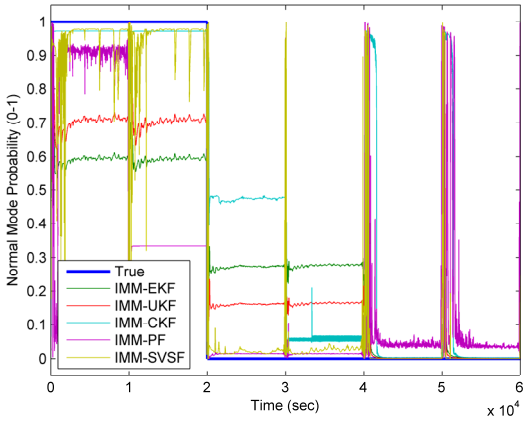

Figure 1. Calculated normal mode probabilities for the EHA.

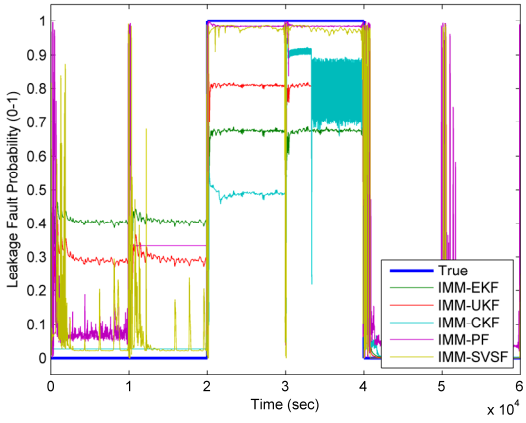

Figure 2. Calculated leakage fault probabilities for the EHA.

All of the strategies successfully detected the correct operating mode (a diagonal probability of 50% or greater); however, with varying results. The IMM-CKF strategy correctly identified the EHA operating normally with the highest probability level (96.82%). The IMM-PF detected the leakage fault with the highest level (97.77%), and the IMM-SVSF correctly identified the friction fault with the highest confidence level (94.10%). It is interesting to note that another important factor to study includes cross-detection errors or misclassifications. For example, during normal operation, the IMM-EKF strategy detected a leakage fault with 40.51% probability. This is a high cross-detection error, as the IMM-EKF method detected normal operation with only 59.31% probability. If these values were even closer, it would be difficult to properly diagnosis the fault with a high level of confidence.

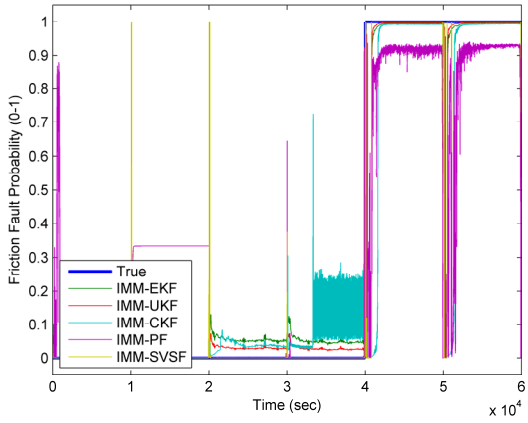

Figure 3. Calculated friction fault probabilities for the EHA.

Another interesting factor to study includes the overall correct detection probability. This can be studied by referring to the confusion matrices and Fig. 4. The summation of the diagonal elements in the matrices yields the total mode probability. Ideally, the perfect detection strategy would correctly identify the operating modes and thus the total mode probability would be 3 or 300%. Overall, the IMM-SVSF provided the best results based on maximizing the correct mode detection and minimizing the misclassifications. The IMM-SVSF had a total mode probability of 283.86%, followed by the IMM-CKF strategy which had 247.83%. This is an improvement of 36.02% (or about 12% per mode) over the second-best strategy.

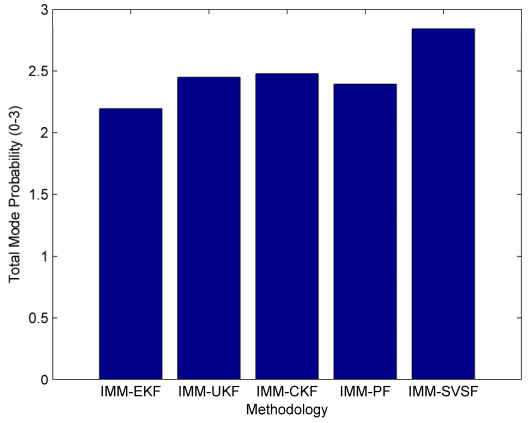

Figure 4. Overall correct detection probability for the compared IMM strategies.

Compared with other popular IMM methods, it appears that the IMM-SVSF provides the best strategy for detecting and diagnosing faults. This may be due to the unique SVSF gain calculation, which yields a robust estimation process [8]. A byproduct of the SVSF gain, as previously discussed, is the chattering phenomenon. This chattering is visible when studying the probability values of the IMM-SVSF strategy in Figs. 1-3.

CONCLUSIONS

Successful fault detection and diagnosis is important for the reliable operation and control of mechatronic engineering systems. This paper studied and compared a number of different model-based strategies, applied on an EHA which was built for experimentation. The results indicated that although all of the strategies were able to successful identify and detect the operating conditions, the IMM-SVSF yielded the most reliable results. The IMM-SVSF successfully identified each condition with over a 90% probability, and minimized unwanted misclassifications. Future research work will study other types of condition monitoring strategies, such as those based on artificial intelligence.

REFERENCES

[1] R. Isermann, Fault Diagnosis Systems, Berlin: Springer-Verlag, 2006.

[2] G. Vachtsevanos, F. Lewis, M. Roemer, A. Hess and B. Wu, Intelligent Fault Diagnosis and Prognosis for Engineering Systems, John Wiley and Sons, Inc., 2006.

[3] M. Basseville and I. Nikiforov, Detection of Abrupt Changes: Theory and Application, Engelwood Cliffs: Prentice-Hall, 1993.

[4] E. Sobhani-Tehrani and K. Khorasani, Fault Diagnosis of Nonlinear Systems Using a Hybrid Approach, Berlin: Springer-Verlag, 2009.

[5] M. Blanke, M. Kinnaert, J. Lunze and M. Staroswiecki, Diagnosis and Fault-Tolerant Control, Berlin: Springer-Verlag, 2006.

[6] Q. Yang, "Model-based and data driven fault diagnosis methods with applications to process monitoring," 2004.

[7] M. A. Al-Shabi, "The Genral Toeplitz/Observability Smooth Variable Structure Filter," 2011.

[8] S. A. Gadsden, "Smooth Variable Structure Filtering: Theory and Applications," Hamilton, Ontario, 2011.

[9] J. Gertler, "Survey of model-based failure detection and isolation in complex plants," *IEEE Control System Magazine,* vol. 8, no. 6, pp. 3-11, 1988.

[10] M. Basseville, "Detecting changes in signals and systems - a survey," *Automatica,* vol. 24, no. 3, pp. 309-326, 1988.

[11] R. Milne, "Strategies for diagnosis," *IEEE Transactions on System, Man, and Cybernetics,* vol. 17, no. 3, pp. 333-339, 1987.

[12] P. M. Frank, "Analytical and qualitative model-based fault diagnosis - a survey and some new results," *European Journal of Control,* vol. 1, no. 2, pp. 26-28, 1996.

[13] P. M. Frank, "Fault diagnosis in dynamic systems using analytical and knowledge based redundancy - a survey and new results," *Automatica,* vol. 26, no. 3, pp. 459-474, 1990.

[14] A. S. Willsky, "A survey of design methods for failure detection in dynamic systems," *Automatica,* vol. 12, no. 6, pp. 601-611, 1976.

[15] R. Isermann, "Process fault detection based on modeling and estimation methods - a survey," *Automatica,* vol. 20, no. 4, pp. 387-404, 1984.

[16] I. Hwang, S. Kim, Y. Kim and C. H. Seah, "A survey of fault detection, isolation, and reconfiguration methods," *IEEE Transactions on Control Systems Technology,* vol. 18, no. 3, pp. 636-653, 2010.

[17] R. Isermann, "Supervision, fault-detection and fault diagnosis methods, an introduction," *Control Engineering Practice,* vol. 2, no. 3, pp. 639-652, 1997.

[18] R. J. Patton, "Fault detection and diagnosis in aerospace systems using analytical redundancy," *IEE Computing & Control Engineering,* vol. 2, no. 3, pp. 127-136, 1990.

[19] R. E. Kalman, "A New Approach to Linear Filtering and Prediction Problems," *Journal of Basic Engineering, Transactions of ASME,* vol. 82, pp. 35-45, 1960.

[20] R. Kalman and R. Bucy, "New Results in Linear Filtering and Prediction Theory," *ASME Journal of Basic Engineering,* vol. 83, pp. 95-108, March 1961.

[21] B. Ristic, S. Arulampalam and N. Gordon, Beyond the Kalman Filter: Particle Filters for Tracking Applications, Boston: Artech House, 2004.

[22] S. R. Habibi, "The Smooth Variable Structure Filter," *Proceedings of the IEEE,* vol. 95, no. 5, pp. 1026-1059, 2007.

[23] S. A. Gadsden and M. Al-Shabi, "The Sliding Innovation Filter," *IEEE Access,* vol. 8, pp. 96129-96138, 2020.

[24] Y. Bar-Shalom, X. Rong Li and T. Kirubarajan, Estimation with Applications to Tracking and Navigation, New York: John Wiley and Sons, Inc., 2001.

[25] S. M. Aly, R. El Fouly and H. Braka, "Extended Kalman filtering an dinteracting multiple model for tracking maneuvering targets in sensor networks," in *IEEE 17th Workshop on Intelligent Solution in Embedded Systems*, 2009.

[26] X. Wang and V. L. Syrmos, "Interacting multiple particle filters for fault diagnosis of nonlinear systems," in *American Control Conference*, Seattle, 2008.

[27] R. Guo, Z. Qin, Q. Li and J. Chen, "Interacting multiple model particle-type filtering approaches to ground target tracking," *Journal of Computers,* vol. 3, no. 7, pp. 23-29, 2008.

[28] S. A. Gadsden, S. R. Habibi and T. Kirubarajan, "A novel interacting multiple model method in target tracking," in *13th Conference on Information Fusion*, Edinburg, UK, 2010.

[29] H. Dang, C. Han and D. Gruyer, "Combining of IMM filtering and DS data association for multi-target tracking," in *7th Conference on Information Fusion*, Stocholm, Sweden, 2004.

[30] S. A. Gadsden, Y. Song and S. R. Habibi, "Novel Model-Based Estimators for the Purposes of Fault Detection and Diagnosis," *IEEE/ASME Transactions on Mechatronics,* vol. 18, no. 4, 2013.

[31] X. Rong Li and Y. Bar-Shalom, "Performance prediction of the interacting Multiple Model algorithm," *IEEE Transactions on Aerospace and Electronic Systems,* vol. 29, no. 3, pp. 755-771, 1993.

[32] M. S. Grewal and A. P. Andrews, Kalman Filtering: Theory and Practice Using MATLAB, 3 ed., New York: John Wiley and Sons, Inc., 2008.

[33] D. Simon, Optimal State Estimation: Kalman, H-Infinity, and Nonlinear Approaches, Wiley-Interscience, 2006.

[34] G. Welch and G. Bishop, "An Introduction to the Kalman Filter," 2006.

[35] S. Julier, "The Spherical Simplex Unscented Transformation," in *Proceedings of the American Conference Conference*, 2003.

[36] S. J. Julier and J. K. Uhlmann, "Unscented Filtering and Nonlinear Estimation," *Proceedings of the IEEE,* vol. 92, no. 3, pp. 401-422, March 2004.

[37] S. J. Julier, J. K. Ulhmann and H. F. Durrant-Whyte, "A New Method for Nonlinear Transformation of Means and Covariances in Filters and Estimators," *IEEE Transactions on Automatic Control,* vol. 45, pp. 472-482, March 2000.

[38] I. Arasaratnam and S. Haykin, "Cubature Kalman Filters," *IEEE Transactions on Automatic Control,* vol. 54, no. 6, June 2009.

[39] S. A. Gadsden and S. R. Habibi, "A New Robust Filtering Strategy for Linear Systems," *ASME Journal of Dynamic Systems, Measurements and Control,* vol. 135, no. 1, January 2013.

[40] S. A. Gadsden, "Smooth Variable Structure Filtering: Theory and Applications," McMaster University, Hamilton, 2011.

[41] S. A. Gadsden and T. Kirubarajan, "Development of a variable structure-based fault detection and diagnosis strategy applied to an electromechanical system," *Proceedings of SPIE 10200, Signal Processing, Sensor/Information Fusion, and Target Recognition ,* vol. XXVI, 2017.